

The Full Range of Predictions for B Physics From Iso-singlet Down Quark Mixing

Dennis Silverman

Department of Physics and Astronomy,

University of California, Irvine

Irvine, CA 92697-4575

(September 7, 2018)

Abstract

We extend the range of predictions of the isosinglet (or vector) down quark model to the fully allowed physical ranges, and also update this with the effect of new physics constraints. We constrain the present allowed ranges of $\sin(2\beta)$ and $\sin(2\alpha)$, γ , x_s , and A_{B_s} . In models allowing mixing to a new isosinglet down quark (as in E_6) flavor changing neutral currents are induced that allow a Z^0 mediated contribution to $B - \bar{B}$ mixing and which bring in new phases. In (ρ, η) , $(x_s, \sin(\gamma))$, and (x_s, A_{B_s}) plots for the extra isosinglet down quark model which are herein extended to the full physical range, we find new allowed regions that will require experiments on $\sin(\gamma)$ and/or x_s to verify or to rule out an extra down quark contribution.

I. INTRODUCTION

The “new physics” class of models we use are those with extra iso-singlet down quarks, where we take only one new down quark as mixing significantly. An example is E_6 , where there are two down quarks for each generation with only one up quark, and of which we assume only one new iso-singlet down quark mixes strongly. This model has shown large possible effects in $B - \bar{B}$ mixing phases. The approaching B factory experiments will also set limits on the phases of the mixing angles to the new iso-singlet down quark in this model. In previous analyses [1,2], we focused on ranges of variables in which the standard model (SM) results occurred, in the sense of looking for small deviations in setting limits. As emphasized by Wolfenstein [3], we now explore the full range of output in variables η , $\sin(\gamma)$, and the B_s asymmetry to indicate the full possible range of outcomes for these experiments due to new physics models.

A significant number of improved constraints have appeared in the last two years, and most importantly, some of the R_b experiments now give results in agreement with the standard model. Since the mixing to a new down quark can only decrease the diagonal neutral current, these results now give useful limits on the parameters. The other improved experiments are $K^+ \rightarrow \pi^+ \nu \bar{\nu}$, the new D0 limit on $B \rightarrow \mu \mu X$, improved V_{ub} limits, and the LEP lower bounds on Δm_s or x_s . We also now have an exact method of combining the one event Poisson result on $K^+ \rightarrow \pi^+ \nu \bar{\nu}$ with the Gaussian probability experiments which results in a chi-squared distribution [4].

We also project to a range of results from the B factory experiments. For different $\sin(2\alpha)$ cases we find extended multiple regions in (ρ, η) that will require experiments on $\sin(\gamma)$ or x_s to decide between, and experiments on both could be required to effectively bound out or to verify the model. We also find a sizeable range for the $B_s - \bar{B}_s$ mixing asymmetry in the extra down quark model, while in the SM this asymmetry is very small. In setting limits we use the method of a joint χ^2 fit to all constraining experiments.

II. ISO-SINGLET DOWN QUARK MIXING MODEL

Groups such as E_6 with extra $SU(2)_L$ singlet down quarks give rise to flavor changing neutral currents (FCNC) through the mixing of four or more down quarks [2,5–8]. We use the 4×4 down quark mixing matrix V which diagonalizes the initial down quarks (d_{iL}^0) to the mass eigenstates (d_{jL}) by $d_{iL}^0 = V_{ij}d_{jL}$. The flavor changing neutral currents we have are [7,8] $-U_{ds} = V_{4d}^*V_{4s}$, $-U_{sb} = V_{4s}^*V_{4b}$, and $-U_{bd} = V_{4b}^*V_{4d}$. These FCNC with tree level Z^0 mediated exchange may contribute part of $B_d^0 - \bar{B}_d^0$ mixing and of $B_s^0 - \bar{B}_s^0$ mixing, and the constraints leave a range of values for the fourth quark's mixing parameters. $B_d^0 - \bar{B}_d^0$ mixing may occur by the $b - \bar{d}$ quarks in a \bar{B}_d annihilating to a virtual Z through a FCNC with amplitude U_{db} , and the virtual Z then creating $\bar{b} - d$ quarks through another FCNC, again with amplitude U_{db} , which then becomes a B_d meson. If these are a large contributor to the $B_d - \bar{B}_d$ mixing, they introduce three new mixing angles and two new phases over the standard model (SM) into the CP violating B decay asymmetries. The size of the contribution of the FCNC amplitude U_{db} as one side of the unitarity quadrangle is less than 0.15 of the unit base $|V_{cd}V_{cb}|$ at the $1\text{-}\sigma$ level, but we have found [2,5,7,8] that it can contribute, at present, as large an amount to $B_d - \bar{B}_d$ mixing as does the standard model. The new phases can appear in this mixing and give total phases different from that of the standard model in CP violating B decay asymmetries [7–11].

For $B_d - \bar{B}_d$ mixing with the four down quark induced $b - d$ coupling, U_{db} , we have [9]

$$x_d = (2G_F/3\sqrt{2})B_B f_B^2 m_B \eta_B \tau_B \left| U_{std-db}^2 + U_{db}^2 \right| \quad (2.1)$$

where with $y_t = m_t^2/m_W^2$

$$U_{std-db}^2 \equiv (\alpha/(4\pi \sin^2 \theta_W)) y_t f_2(y_t) (V_{td}^* V_{tb})^2, \quad (2.2)$$

and $x_d = \Delta m_{B_d}/\Gamma_{B_d} = \tau_{B_d} \Delta m_{B_d}$.

The CP violating decay asymmetries depend on the combined phases of the $B_d^0 - \bar{B}_d^0$ mixing and the b quark decay amplitudes into final states of definite CP . Since we have

found that Z mediated FCNC processes may contribute significantly to $B_d^0 - \bar{B}_d^0$ mixing, the phases of U_{db} would be important. Calling the singlet down quark D , to leading order the mixing matrix elements to D are $V_{tD} \approx s_{34}$, $V_{cD} \approx s_{24}e^{-i\delta_{24}}$, and $V_{uD} \approx s_{14}e^{-i\delta_{14}}$. The complete 4×4 mixing matrix was given previously [9,12]. The FCNC amplitude U_{db} to leading order in the new angles is

$$U_{db} = (-s_{34} - s_{24}s_{23}e^{i\delta_{24}})(s_{34}V_{td}^* + s_{14}e^{-i\delta_{14}} - s_{24}e^{-i\delta_{24}}s_{12}). \quad (2.3)$$

where $V_{td} \approx (s_{12}s_{23} - s_{13}e^{i\delta_{13}})$, and $V_{ub} = s_{13}e^{-i\delta_{13}}$.

III. JOINT CHI-SQUARED ANALYSIS FOR CKM AND FCNC EXPERIMENTS

FCNC experiments put limits on the new mixing angles and constrain the possibility of new physics contributing to $B_d^0 - \bar{B}_d^0$ and $B_s^0 - \bar{B}_s^0$ mixing. Here we jointly analyze all constraints on the 4×4 mixing matrix obtained by assuming only one of the $SU(2)_L$ singlet down quarks mixes appreciably [7]. We use the nine experiments for the 3×3 CKM sub-matrix elements [1], which include: those on the five matrix elements $V_{ud}, V_{cd}, V_{us}, V_{ub}, V_{cb}$ of the u and c quark rows; $|\epsilon|$ and $K_L \rightarrow \mu\mu$ in the neutral K system [13]; $B_d - \bar{B}_d$ mixing (x_d); and the new limits on Δm_s , or x_s . For studying FCNC, we have four experiments which include the bound on $B \rightarrow \mu\mu X$ (which constrains $b \rightarrow d$ and $b \rightarrow s$) for which we have the UA1 and the new D0 [14] results, the new first event in $K^+ \rightarrow \pi^+\nu\bar{\nu}$ [4,11,15–17] and new results on R_b in $Z^0 \rightarrow b\bar{b}$ [11,18] (which directly constrains the V_{4b} mixing element). FCNC experiments will bound the three amplitudes U_{ds}, U_{sb} , and U_{bd} which contain three new mixing angles and three phases. We use the mass of the top quark as $m_t = 174$ GeV. We use a method for combining the Bayesian Poisson distribution for the average for the one observed event in $K^+ \rightarrow \pi^+\nu\bar{\nu}$ [17] with the chi-squared distribution from the other experiments. We take $\langle n \rangle = 2.7 \times 10^8 |U_{ds}|^2$, ignoring the SM contribution since the observed event is at a rate four times the SM result.

In maximum likelihood correlation plots, we use for axes two output quantities which are dependent on the mixing matrix angles and phases, such as (ρ, η) , and for each possible

bin with given values for these, we search through the nine dimensional angular data set of the 4×4 down quark mixing angles and phases, finding all sets which give results in the bin, and then put into that bin the minimum χ^2 among them. To present the results, we then draw contours at several χ^2 in this two dimensional plot corresponding to given confidence levels.

IV. CONSTRAINTS ON THE STANDARD MODEL CKM MATRIX AT PRESENT

We first analyze the standard model using the present constraints on the eight CKM related experiments. We use the results for $|V_{ub}/V_{cb}| = 0.08 \pm 0.016$ or a 20% error [19].

In Fig. 1 is shown the (ρ, η) plot for the standard model with contours at χ^2 which correspond to confidence levels (CL) that are the same as the CL for 1- σ , 2- σ , and 3- σ limits. Fig. 1 shows large regions for the present CKM constraints. We see the effects of the $x_s = 1.35x_d|V_{ts}/V_{td}|^2$ lower bound in the SM limiting the length of $V_{td} \propto \sqrt{(1 - \rho)^2 + \eta^2}$ and starting to cut off ρ for $\rho < 0$.

In Fig. 2 is shown the $(\sin(2\alpha), \sin(2\beta))$ plot for the standard model, for the same cases as in Fig. 1. In comparison to previous analyses [2] the region near $\sin(2\alpha) = 1$ is no longer within the 1- σ contour.

In Fig. 3 is shown the $(x_s, \sin(\gamma))$ plot for the standard model with (a) present data, and (b) for the B factory cases $\sin(2\alpha) = 1, 0, -1$ from left to right. x_s is determined in the SM from $x_s = 1.35x_d(|V_{ts}|/|V_{td}|)^2$. The largest errors arise from the uncertainty in $|V_{td}|$, which follow from the present 20% uncertainty in $\sqrt{B_B}f_B = 200 \pm 40$ MeV from lattice calculations [21]. The B factory in the SM constructs a rigid triangle from the knowledge of α and β , and removes this uncertainty in γ and x_s in the future. A cautionary note for experiments emerges from this plot, namely that $\sin(\gamma)$ is close to one (0.7 to 1.0) for the 1- σ contour, and high accuracy on $\sin(\gamma)$ will be needed to add new information to the standard model. At 1- σ the range of x_s in the standard model is from 14 to 33. It is clear that the different

$\sin(2\alpha)$ cases gives distinct ranges for x_s . Checking whether x_s agrees with the range given by a $\sin(2\alpha)$ measurement will be a good test of the standard model.

V. CONSTRAINTS ON THE FOUR DOWN QUARK MODEL AT PRESENT, AND AFTER THE B FACTORY RESULTS

In the following, we will find and take $\sin(2\beta) = 0.65$ as the center of the current range for the SM with its projected B factory errors of ± 0.06 [22], and vary $\sin(2\alpha)$ from -1.0 to 1.0 , using the projected B factory errors of ± 0.08 .

Here we also project forward to having results on $\sin(2\alpha)$ and $\sin(2\beta)$ from the B factories, and show how there will be stronger limits on the new phases of FCNC couplings than from present data. In the four down quark model we use “ $\sin(2\alpha)$ ” and “ $\sin(2\beta)$ ” to denote results of the appropriate B_d decay CP violating asymmetries, but since the mixing amplitude is a superposition, the experimental results for these asymmetries are not directly related to angles in a triangle in this model. The asymmetries with FCNC contributions included are

$$\sin(2\beta) \equiv A_{B_d^0 \rightarrow \Psi K_s^0} = \text{Im} \left[\frac{(U_{std-db}^2 + U_{db}^2) (V_{cb}^* V_{cs})}{|U_{std-db}^2 + U_{db}^2| (V_{cb}^* V_{cs})^*} \right] \quad (5.1)$$

$$\sin(2\alpha) \equiv -A_{B_d^0 \rightarrow \pi^+ \pi^-} = -\text{Im} \left[\frac{(U_{std-db}^2 + U_{db}^2) (V_{ub}^* V_{ud})}{|U_{std-db}^2 + U_{db}^2| (V_{ub}^* V_{ud})^*} \right] \quad (5.2)$$

with U_{std-db} defined in Eqn. (2.2).

In the four down quark model, what we mean by “ $\sin(\gamma)$ ” is the result of the experiments which would give this variable in the SM [23]. Here, the four down quark model involves more complicated amplitudes, and $\sin(\gamma)$ is not simply $\sin(\delta_{13})$:

$$\sin(\gamma) \equiv \text{Im} \left[\frac{(U_{std-bs}^2 + U_{bs}^2) (V_{ub}^* V_{cs})}{|U_{std-bs}^2 + U_{bs}^2| |V_{ub} V_{cs}|} \right]. \quad (5.3)$$

We note that since $\sin(\gamma)$ is an imaginary part of a complex amplitude, it can have values ranging from -1 to $+1$. We now extend the range of the previous analyses to cover the complete range.

In the four down quark model, x_s is no longer the simple ratio of two CKM matrix elements, but now involves the Z -mediated annihilations and exchange amplitudes as well

$$x_s = 1.35x_d \frac{|U_{std-bs}^2 + U_{bs}^2|}{|U_{std-db}^2 + U_{db}^2|}, \quad (5.4)$$

where

$$U_{std-bs}^2 = (\alpha/(4\pi \sin^2 \theta_W)) y_t f_2(y_t) (V_{tb}^* V_{ts})^2. \quad (5.5)$$

The asymmetry A_{B_s} in B_s mixing in the standard model with the leading decay process of $b \rightarrow c\bar{c}s$ has no significant phase from the decay or from the mixing which is proportional to V_{ts}^2 . The near vanishing of this asymmetry is a test of the standard model [6], and a non-zero value can result from a ‘‘new physics’’ model. With the FCNC, the result is

$$A_{B_s} = \text{Im} \left[\frac{(U_{std-bs}^2 + U_{bs}^2) (V_{cb}^* V_{cs})}{|U_{std-bs}^2 + U_{bs}^2| (V_{cb}^* V_{cs})^*} \right] \quad (5.6)$$

Again, since this is an imaginary part of a complex amplitude, we extend our studies to the full range including negative values for this. Since it concerns the B_s mixing, we plot it against x_s which involves the magnitude of the amplitude used in A_{B_s} .

In the four-down-quark model with the unitarity quadrangle, what we plot for the (ρ, η) plot is the scaled vertex of the matrix element V_{ub}^*

$$\rho + i\eta \equiv V_{ub}^* V_{ud} / |V_{cb} V_{cs}|. \quad (5.7)$$

Since η is an imaginary part, it can have negative as well as positive values. While the negative values were not included before in comparing to the standard model, they are now included to show the full range of predictions of the four-down-quark model.

We then make maximum likelihood plots which include $(\sin(2\alpha), \sin(2\beta))$, (ρ, η) , $(x_s, \sin \gamma)$, and (x_s, A_{B_s}) .

The corresponding plots for the four down quark model are shown for present data and for projected B factory data in the following figures. In the figures, we show χ^2 contour plots with confidence levels (CL) at values equivalent to $1\text{-}\sigma$ and at 90% CL (1.64σ) for

present data, and for projected B factory results. Again, for results with the B factories, we use the example of the most likely $\sin(2\beta) = 0.65$ with B factory errors of ± 0.06 , and errors of ± 0.08 on $\sin(2\alpha)$.

In Fig. 4 we have plotted the χ^2 contours for the location of the vertex of (ρ, η) . We note that in contrast to the standard model, in Fig. 4a the presently allowed 90% CL contour in the four down quark model is an annular ring representing no constraint on $\delta = \delta_{13}$ which can result from the FCNC with its new phases $e^{i\delta_{14}}$ or $e^{i\delta_{24}}$ in U_{db} causing the known CP violation. In Fig. 4b,c and d we show the B factory cases of $\sin(2\alpha) = -1, 0$ and 1 , respectively, with contours at $1-\sigma$ and at 90% CL. The existence of several regions, even now for negative η , requires that extra experiments in $\sin(\gamma)$ or x_s will also be needed to verify or to bound out the extra down quark mixing model. Use of the slightly more conservative bound for $|V_{ub}/V_{cb}|$ of 0.08 ± 0.02 , which is used by some authors, still results in multiple regions.

In order to display how the FCNC Z^0 exchange with the new phases in U_{ds} can account for the CP violation in ϵ_K , we plot the ratio of the FCNC contribution to the root-mean-square of the SM and the FCNC contributions,

$$R_\epsilon^{\text{FCNC}} = \frac{\text{Im}(U_{ds}^2)}{((A_\epsilon^{\text{SM}})^2 + (\text{Im}(U_{ds}^2))^2)^{1/2}}, \quad (5.8)$$

so that $-1 \leq R_\epsilon^{\text{FCNC}} \leq 1$. Here $A_\epsilon^{\text{SM}} = \alpha \text{Im}(-\tilde{E}^*) / (4\pi \sin^2 \theta_W)$ and E is from Inami and Lim [20]. In Fig. 5 R_ϵ^{FCNC} is shown against the angle of V_{ub}^* which is δ_{13} . In Fig. 5, for δ_{13} from 20° to 150° , $R_\epsilon^{\text{FCNC}} = 0$ is allowed, i.e., the SM can account for ϵ_K in this analysis. At angles further outside that region, for $-180 \leq \delta_{13} \leq 0$, only new physics contributions can give the imaginary part, where $R_\epsilon^{\text{FCNC}} \approx 1$.

In computing χ^2 for a $(\sin(2\alpha), \sin(2\beta))$ contour plot for the four down quark model we find that all pairs of $(\sin(2\alpha), \sin(2\beta))$ are individually allowed at $1-\sigma$. This is a much broader allowed region in $\sin(2\beta)$ than the standard model result from present data in Fig. 2. The allowed $1-\sigma$, 90% CL and $2-\sigma$ contours in the $(\sin(2\alpha), \sin(2\beta))$ plot for the cases of the B factory results with the four down quark model are very similar to the SM results

shown in Fig. 2.

In terms of other experiments, the $(x_s, \sin(\gamma))$ plot for the four down quark model is shown in Fig. 6a with the allowed region from present data, with $1\text{-}\sigma$ and 90% CL contours. This allows all values of $\sin(\gamma)$ even in the extended region from $-1 \leq \sin(\gamma) \leq 1$ at the 90% CL. At $1\text{-}\sigma$, x_s lies between 13 and 48.

In Figs. 6b, c and d are shown the cases $\sin(2\alpha) = -1, 0$, and 1 , respectively, at $1\text{-}\sigma$ and at 90% CL. They reflect the same regions that appeared in the (ρ, η) plots, Figs. 4b, c, and d. The resemblance is increased if we recall that roughly $\sin(\gamma) \approx \eta$, and also that $x_s \propto x_d/|V_{td}|^2$ where $|V_{td}|$ is the distance from the $\rho = 1, \eta = 0$ point. We see that experiments on $\sin(\gamma)$ and x_s are necessary to resolve the possible regions allowed by the four down quark model. For the case of $\sin(2\alpha) = -1$, the allowed values of $\sin(\gamma)$ in Fig. 6b are different than those for the standard model in Fig. 3a. The $\sin(2\alpha) = 0$ case allows regions of $\sin(\gamma)$ lower than in the SM.

The extent of the non-zero value of A_{B_s} in the four down quark model is shown in Fig. 7 from present data with contours at $1\text{-}\sigma$, $2\text{-}\sigma$, and $3\text{-}\sigma$. Plots for the B factory cases (not shown) are similar. We note that in the new full range plot A_{B_s} is roughly symmetric about zero, with the largest absolute values at 0.35 at $1\text{-}\sigma$, and $0.5 \rightarrow 0.6$ at 90% CL. This is much different from the ≤ 0.025 value of A_{B_s} in the SM.

We now report on additional plots that are not shown here. We compared the limits on the four down quark FCNC amplitude $|U_{db}|$ versus the standard model amplitude $|U_{std-db}|$ for $B_d^0 - \bar{B}_d^0$ mixing, at present and after the B factory results. At present the constraints are such that $|U_{db}|$ can go from zero up to as large as the magnitude of $|U_{std-db}|$ at $1\text{-}\sigma$ [9]. $|U_{sb}|$ is restricted to about half of $|U_{std-bs}|$. The total phase of $B_d^0 - \bar{B}_d^0$ mixing can range over all angles, while the SM phase is between -30° and 80° when in combination with the FCNC amplitude. The magnitude of $|U_{db}/(V_{cd}V_{cb})|$ in the unitarity triangle is ≤ 0.15 at $1\text{-}\sigma$.

The 90% CL limits on the three new quark mixing elements $|V_{4d}|$, $|V_{4s}|$, and $|V_{4b}|$ are roughly equal to the mixing angles to the fourth down quark θ_{14} , θ_{24} and θ_{34} , respectively. They are bounded by 0.05, 0.05, and 0.08, respectively. The values allowed in combination

are much more restricted, since they are roughly bounded by hyperbolic curves, due to constraints acting on their products in U_{ds} , U_{sb} , and U_{bd} .

VI. CONCLUSIONS

We have extended our analysis to the full range of the variables η , $\sin(\gamma)$ and A_{B_s} , all of which are imaginary parts, to include all of their negative values. For the four down quark model they all show remarkable and experimentally important new behaviours. From present constraints, the vertex of V_{ub}^* now is allowed in this model to be complete circular annuli about $(\rho, \eta) = (0, 0)$ at 90% CL due to the new phases δ_{14} or δ_{24} accounting for the presently observed CP violation in ϵ . $\sin(\gamma)$ is now allowed in this model over its entire range from -1 to $+1$. The range of A_{B_s} is almost equally as large for its negative values as it is for its positive values, and perhaps large enough to be observed. Since it is almost null in the SM, this could be a dramatic evidence of new physics.

For the B factory cases there are new multifold allowed regions as shown in the extended (ρ, η) plots including for negative η . This will require additional experiments on x_s and $\sin(\gamma)$ to well define the four down quark model results, and eventually to verify or bound out the relevance of the model here. In the $(x_s, \sin(\gamma))$ plot for similar cases, there are new multiple regions for $\sin(\gamma)$ negative.

ACKNOWLEDGMENTS

This research was supported in part by the U.S. Department of Energy under Contract No. DE-FG0391ER40679. We acknowledge the hospitality of SLAC and CERN. We thank Heng Tony Yao for discussions.

REFERENCES

- [1] W.-S. Choong and D. Silverman, Phys. Rev. D **49**, 2322 (1994). Typographical corrections are changing the signs of U_{sd} and U_{ds} in Eqns. (13) and (36).
- [2] D. Silverman, Int. Journal of Modern Physics **A11** 2253 (1996), hep-ph/9504387.
- [3] Joao P. Silva and L. Wolfenstein, Phys. Rev. D **55**, 5331 (1997), hep-ph/9610208.
- [4] D. Silverman, “Joint Treatment of Poisson and Gaussian Experiments in a Chi-squared Statistic”, U. C. Irvine TR-98-15.
- [5] M. Shin, M. Bander, and D. Silverman, Phys. Lett. **B219**, 381 (1989).
- [6] Y. Nir and D. Silverman, Nucl. Phys. **B345**, 301 (1990).
- [7] Y. Nir and D. Silverman, Phys. Rev. D **42**, 1477 (1990).
- [8] D. Silverman, Phys. Rev. D **45**, 1800 (1992), and references to earlier literature therein.
- [9] W.-S. Choong and D. Silverman, Phys. Rev. D **49**, 1649 (1994).
- [10] G. C. Branco, T. Morozumi, P. A. Parada, and M. N. Rebelo, Phys. Rev. D **48**, 1167 (1993).
- [11] L. Lavoura and J. P. Silva, Phys. Rev. D **47**, 1117 (1993).
- [12] F. J. Botella and L. L. Chau, Phys. Lett. **168B**, 97 (1986); H. Harari and M. Leuler, Phys. Lett. B **181**, 123 (1986).
- [13] Here in $K_L \rightarrow \mu\mu$ the joint error from BNL and KEK is scaled up by a factor of 1.3 using the Particle Data Group method. After subtracting the 2γ unitarity contribution we have $|A_R|^2 = (0.23 \pm 0.54) \times 10^{-9}$. The latest experimental report from BNL is A. P. Heinson *et al.*, Phys. Rev. D **51**, 985 (1995). At $1\text{-}\sigma$, the bound on $|A_R|$ is about the upper limit on the long distance contribution estimates.
- [14] The D0 Collaboration, S. Abachi *et al.*, FERMILAB Conf-96/253-E (1996).

- [15] M. S. Atiya *et al.* Phys. Rev. Lett. **70**, 2521 (1993).
- [16] S. Adler *et al.*, Phys. Rev. Lett. **76**, 1421 (1996).
- [17] S. Adler *et al.*, Phys. Rev. Lett. **79**, 2204 (1997).
- [18] We take the $1\text{-}\sigma$ fractional error on R_b from the deviation of the combined average from the SM result, since if there is a real positive deviation, it would not come from FCNC but from new physics not included here.
- [19] A. Ali and D. London, Nucl. Phys. Proc. Suppl. 54A, 297-308 (1997), hep-ph/9607392.
- [20] T. Inami and C. S. Lim, Prog. Theor. Phys. **65**, 297 (1981).
- [21] S. R. Sharpe, talk given at Lattice 96: 14th International Symposium on Lattice Field Theory, St. Louis, MO, 4-8 Jun 1996. Published in Nucl. Phys. Proc. Suppl. 53:181-198, 1997, also in Lattice 96:181-198 (QCD161:I715:1996), hep-lat/9609029.
- [22] F. Porter and A. Snyder, Babar note No. 140 and B Factory Letter of Intent, SLAC Report 443 (1994).
- [23] R. Aleksan, B. Kayser, and D. London, Proc. of the Workshop on B Physics at Hadron Accelerators, p. 299-308, Snowmass, Colo. 1993, Ed. P. McBride and C. S. Mishra, hep-ph/9312338; R. Aleksan, I. Dunietz, B. Kayser, and F. LeDiberder, Nucl. Phys. **B361**, 1991; R. Aleksan, I. Dunietz, and B. Kayser, Z. Phys. **C54**, 653 (1992).

FIGURES

FIG. 1. The (ρ, η) plot for the standard model, showing the 1, 2, and 3- σ contours, for the present data (large contours) and for projected B factory results (smaller circular contours) at $\sin(2\alpha) = 1, 0$, and -1 from left to right.

FIG. 2. The $(\sin(2\alpha), \sin(2\beta))$ plot for the standard model at 1, 2, and 3- σ with present data (nearly horizontal contours), and with the sample results of the B factories (almost circular contours), for $\sin(2\alpha) = 1, 0$, and -1 from left to right.

FIG. 3. The $(x_s, \sin \gamma)$ plots are shown for the standard model with: (a) present limits; and (b) sample results for the B factories for $\sin(2\alpha) = 1, 0$, and -1 from left to right.

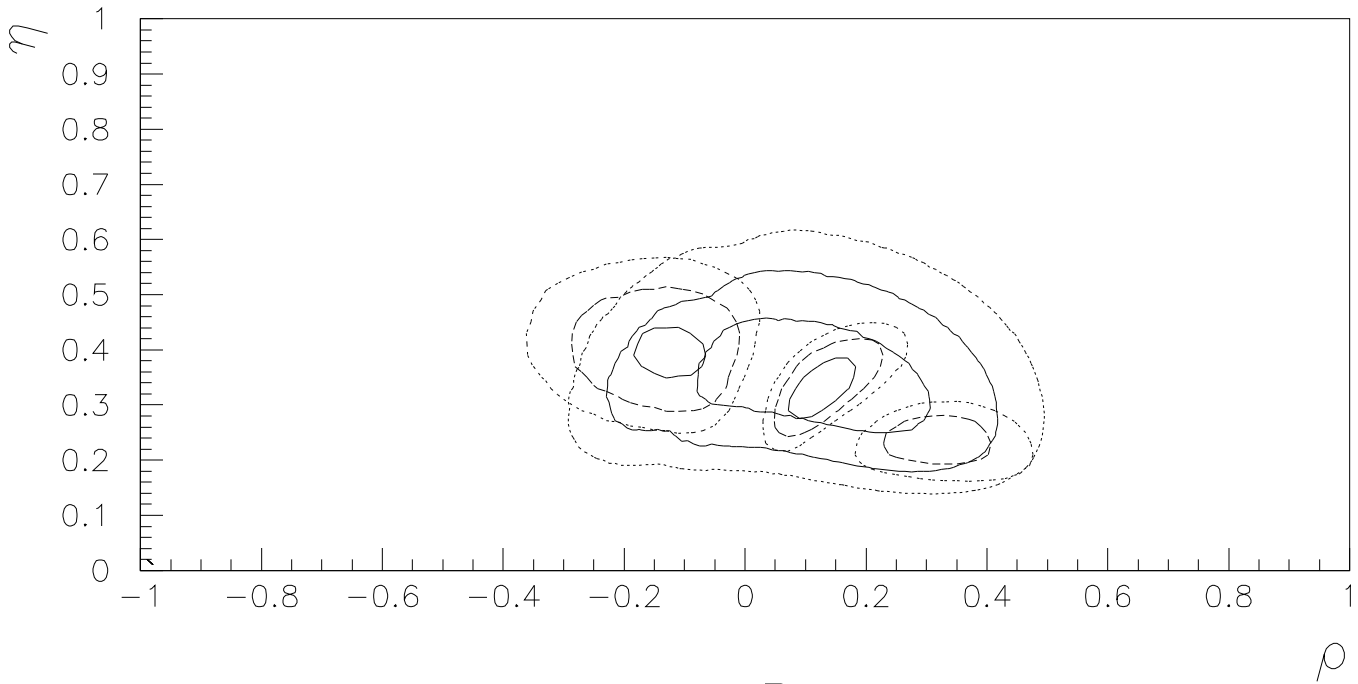
FIG. 4. The (ρ, η) plots for the four down quark model from: (a) present data, and for B factory cases for values of $\sin(2\alpha)$ as labeled. Contours are at 1- σ and at 90% CL.

FIG. 5. The ratio R_ϵ^{FCNC} of the contribution of the FCNC amplitude to ϵ_K divided by the root-mean-square of the SM and the FCNC amplitudes, as a function of the angle δ_{13} .

FIG. 6. The $(x_s, \sin(\gamma))$ plots for the four down quark model from (a) present data, and (b, c, and d) for B factory cases for values of $\sin(2\alpha)$ as labeled. Contours are the same as in Fig. 4.

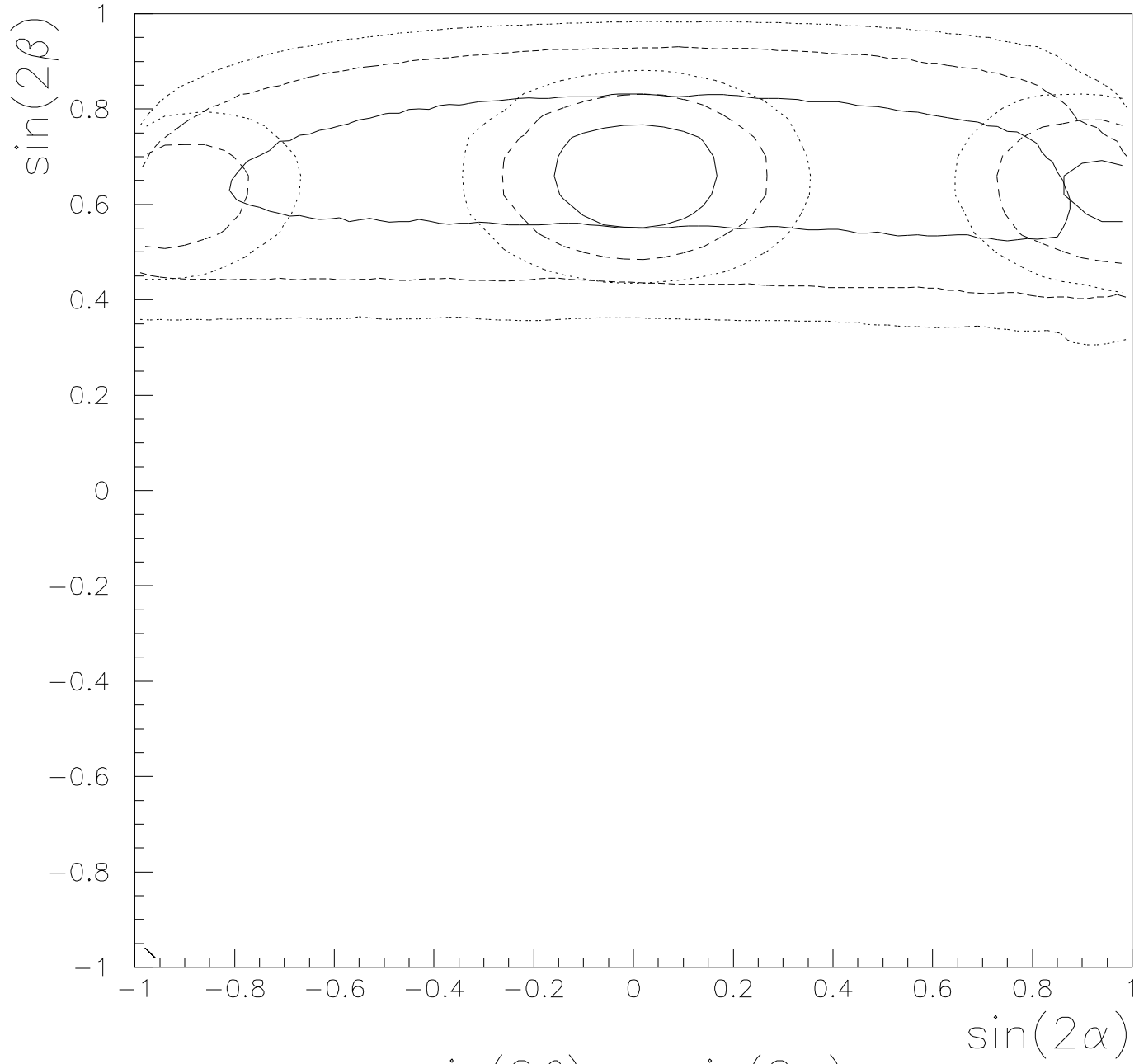
FIG. 7. The (x_s, A_{B_s}) plot for the B_s asymmetry A_{B_s} in the four down quark model for present data, with contours at 1, 2 and 3- σ .

SM: Present, & B Factory $\sin(2\alpha) = 1, 0, -1$



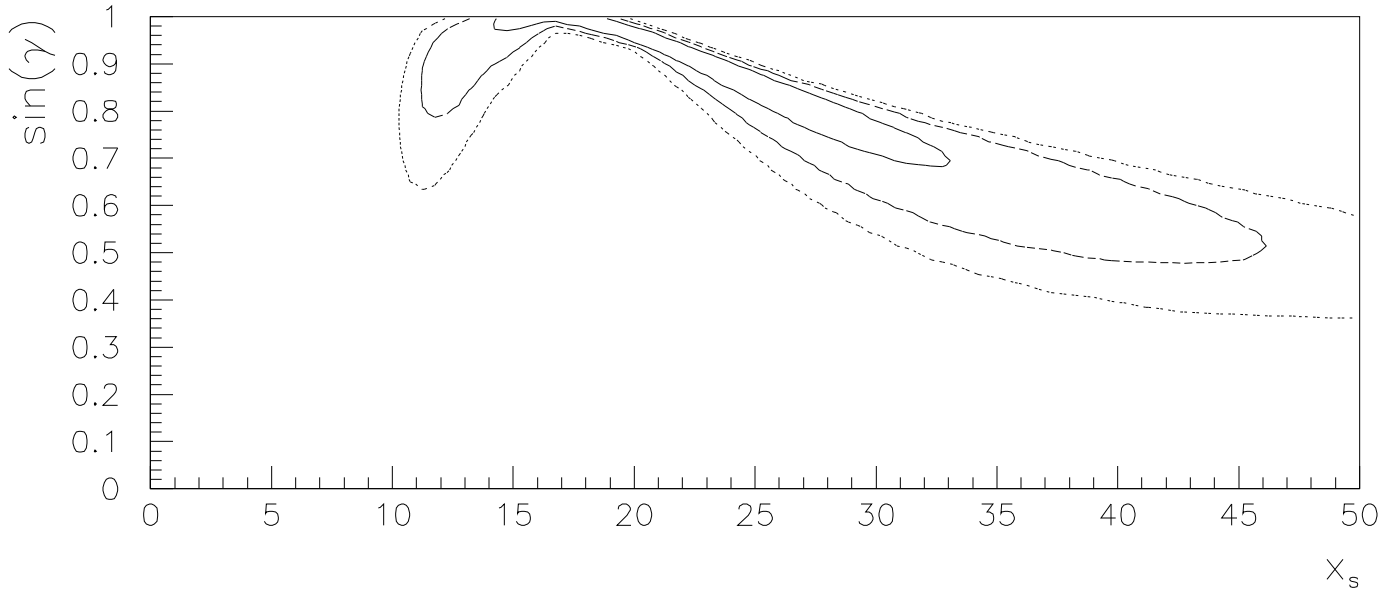
ρ - η Plot

SM: Present, & B Factory $\sin(2\alpha) = -1, 0, 1$

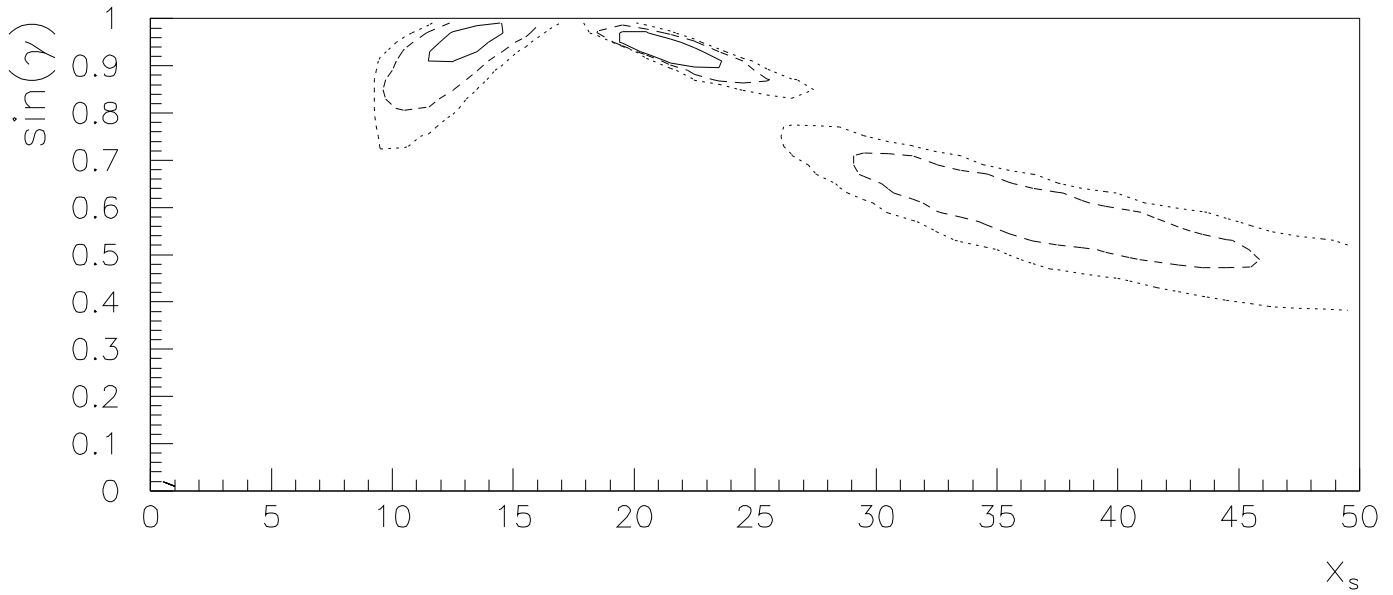


$\sin(2\beta)$ vs. $\sin(2\alpha)$

Standard Model

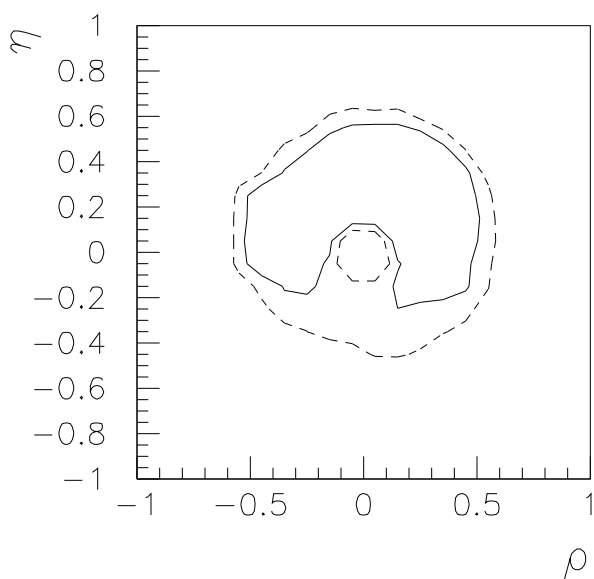


(a) Present Data

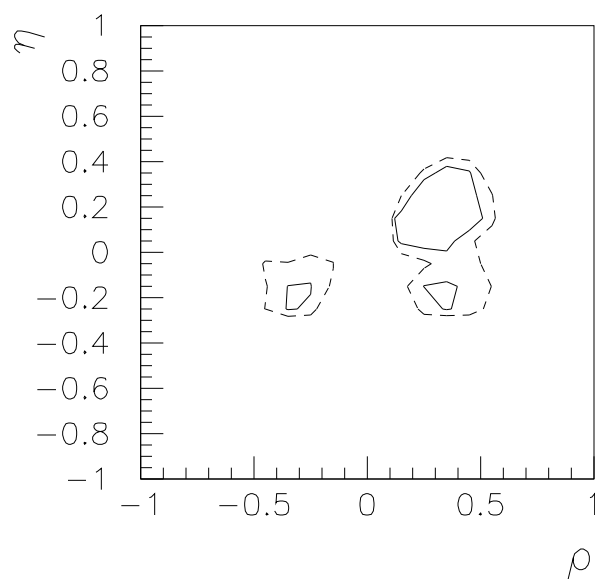


(b) B Factory $\sin(2\alpha) = 1, 0, -1$

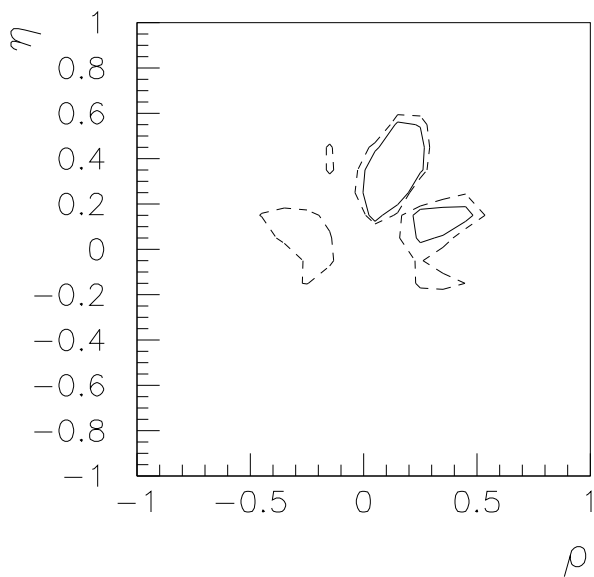
Four Down Quark Model, 1σ , 90%CL



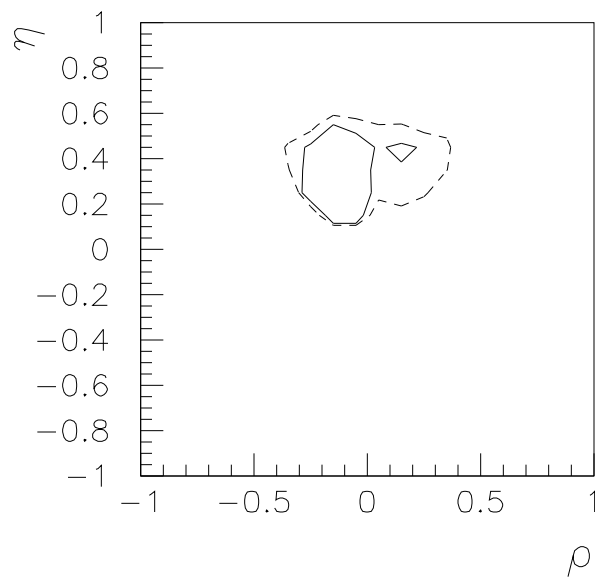
(a) Present



(b) $\sin(2\alpha) = -1$

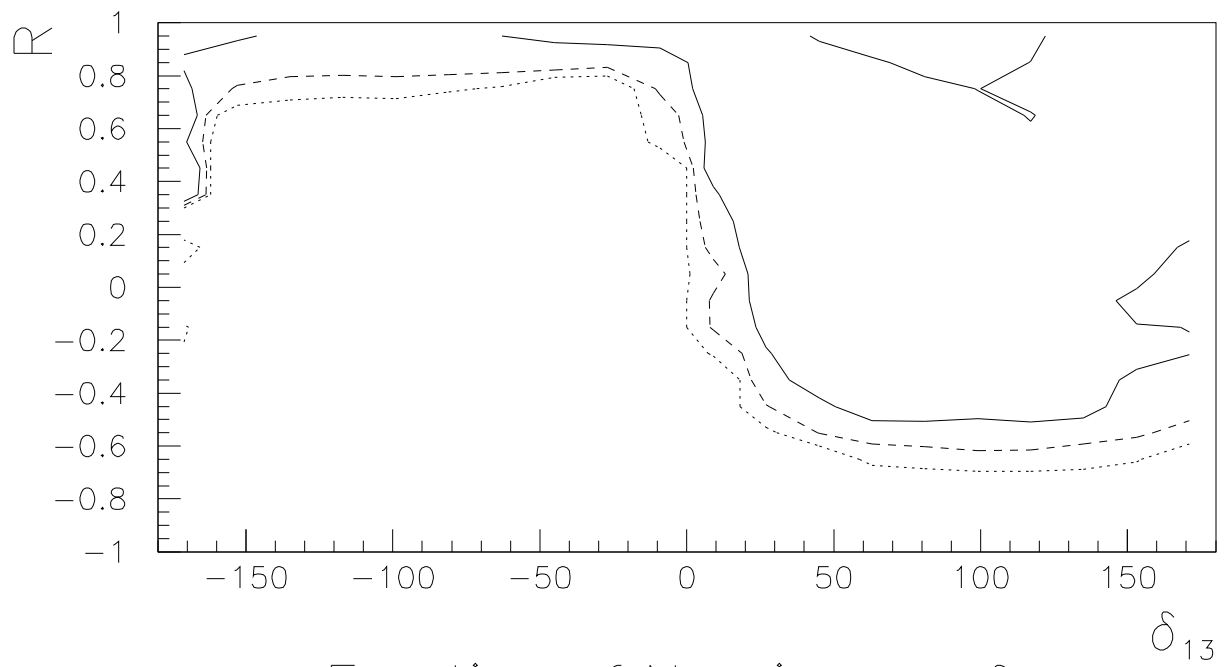


(c) $\sin(2\alpha) = 0$



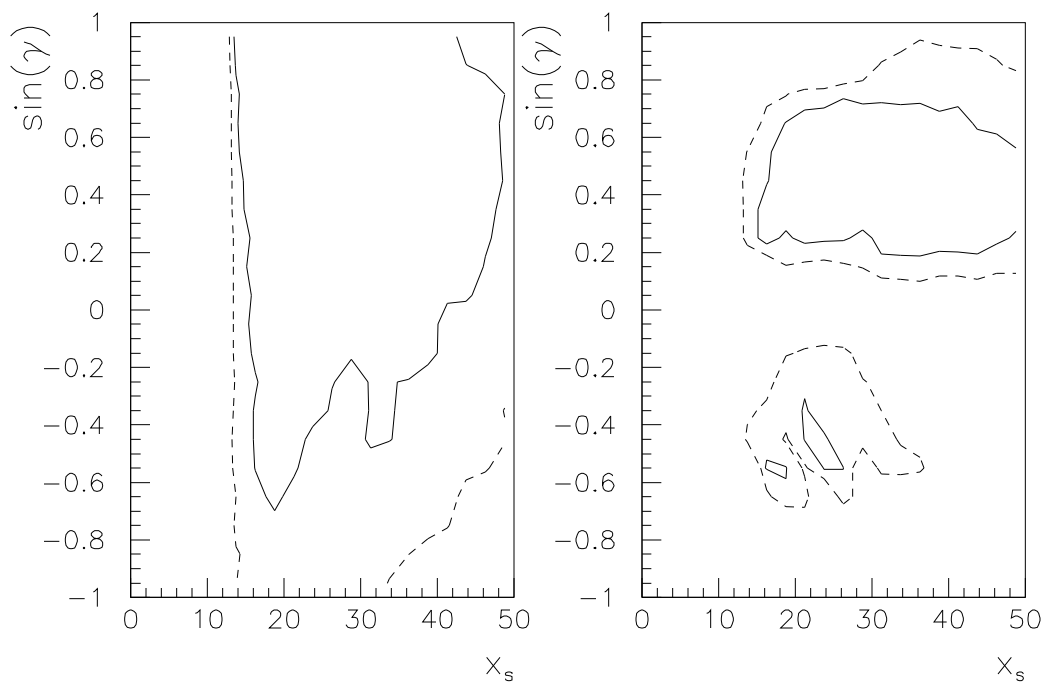
(d) $\sin(2\alpha) = 1$

Four Down Quarks – Present, 1,2,3 σ



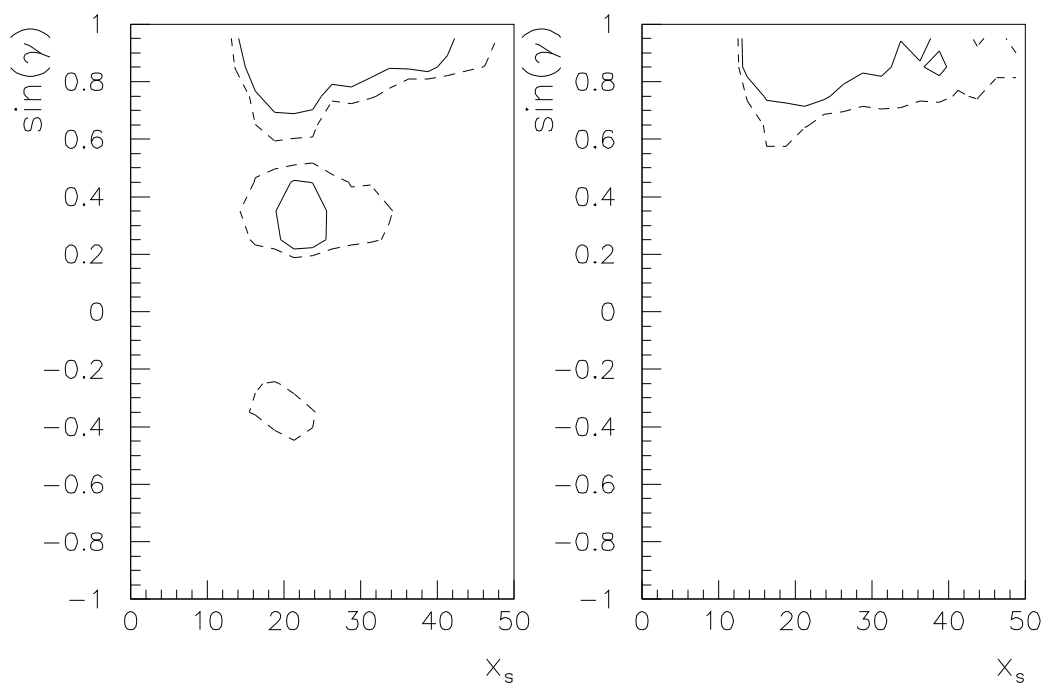
Fraction of New in ε vs. δ_{13}

Four Down Quark Model, 1σ , 90% CL



(a) Present

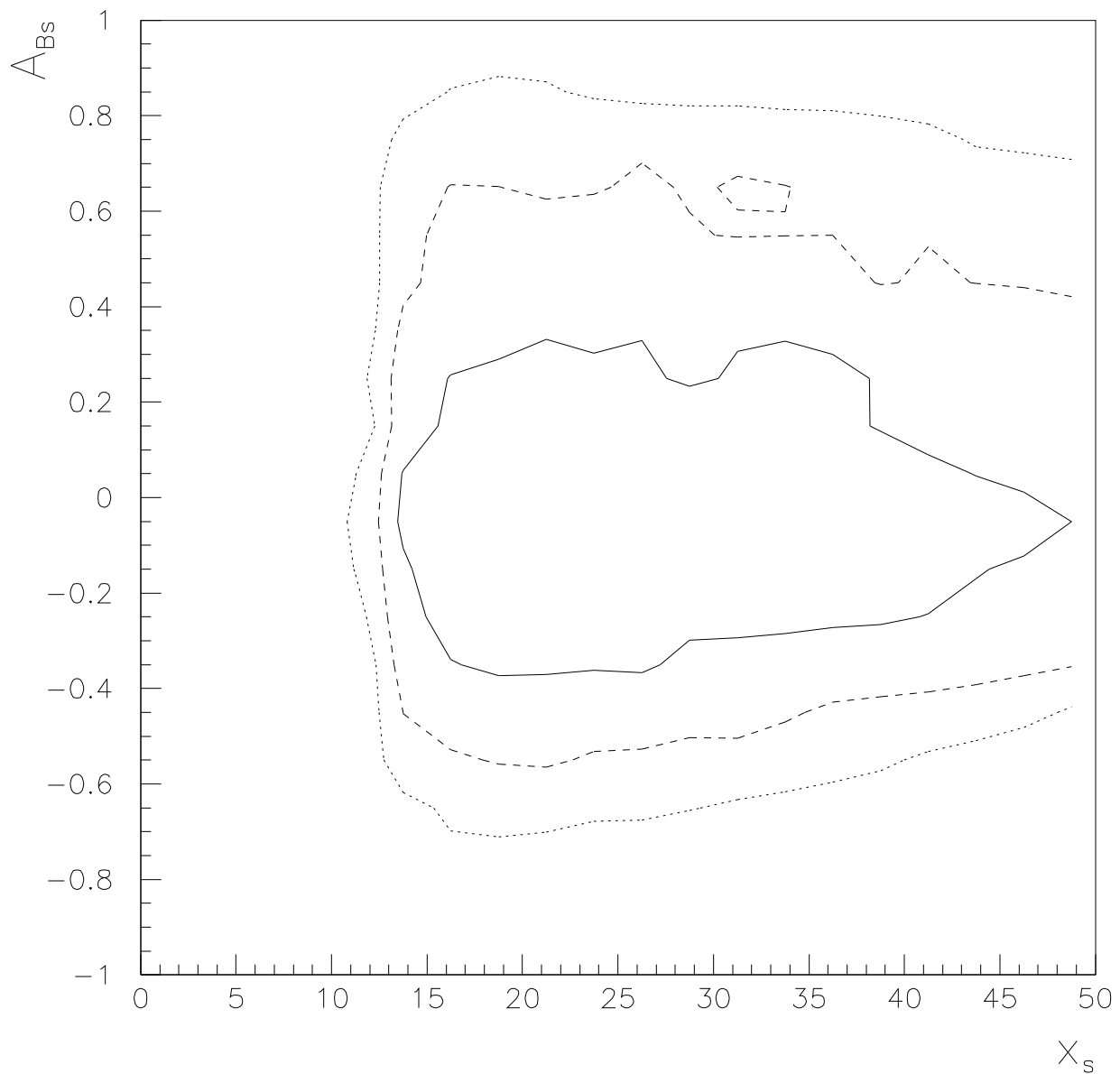
(b) $\sin(2\alpha) = -1$



(c) $\sin(2\alpha) = 0$

(d) $\sin(2\alpha) = 1$

Four Down Quarks – Present, 1,2,3 σ



B_s Mixing Asymmetry vs x_s